Field trial of active remote sensing using a high-power short-wave infrared supercontinuum laser

Vinay V. Alexander,[1,*] Zhennan Shi,[1] Mohammed N. Islam,[1,2] Kevin Ke,[2] Galina Kalinchenko,[2] Michael J. Freeman,[2] Agustin Ifarraguerri,[3] Joseph Meola,[4] Anthony Absi,[4] James Leonard,[4] Jerome A. Zadnik,[5] Anthony S. Szalkowski,[6] and Gregory J. Boer[7]

[1]Electrical and Computer Engineering Department, University of Michigan, Ann Arbor, Michigan 48109, USA

[2]Omni Sciences Inc., Dexter, Michigan 48105, USA

[3]SAIC, Arlington, Virginia 22203, USA

[4]Air Force Research Labs, Wright Patterson Air Force Base, Ohio 45433, USA

[5]EOIR Technologies, Fredericksburg, Virginia 22408, USA

[6]Booz Allen Hamilton Inc., McLean, Virginia 22102, USA

[7]National Geospatial-Intelligence Agency, Springfield, Virginia 22150, USA

*Corresponding author: vinalex@umich.edu

Received 3 July 2013; revised 20 August 2013; accepted 22 August 2013; posted 22 August 2013 (Doc. ID 193055); published 19 September 2013

Field trial results of a 5 W all-fiber broadband supercontinuum (SC) laser covering the short-wave infrared (SWIR) wavelength bands from ~1.55 to 2.35 μm are presented. The SC laser is kept on a 12 story tower at the Wright Patterson Air Force Base and propagated through the atmosphere to a target 1.6 km away. Beam quality of the SC laser after propagating through 1.6 km is studied using a SWIR camera and show a near diffraction limited beam with an M^2 value of <1.3. The SC laser is used as the illumination source to perform spectral reflectance measurements of various samples at 1.6 km, and the results are seen to be in good agreement with in-lab measurements using a conventional lamp source. Spectral stability measurements are performed after atmospheric propagation through 1.6 km and show a relative variability of ~4%–8% across the spectrum depending on the atmospheric turbulence effects. Spectral stability measurements are also performed in-lab and show a relative variability of <0.6% across the spectrum. © 2013 Optical Society of America

OCIS codes: (280.0280) Remote sensing and sensors; (140.3070) Infrared and far-infrared lasers; (300.6340) Spectroscopy, infrared; (320.6629) Supercontinuum generation.

http://dx.doi.org/10.1364/AO.52.006813

1. Introduction

We demonstrate a 5 W all-fiber supercontinuum (SC) laser prototype spanning the short-wave infrared (SWIR) wavelength band from ~1.55–2.35 μm. Field trials are performed using the developed SC laser kept on a 76 m tall tower at the Wright Patterson Air Force Base (WPAFB) and propagated through the atmosphere to a target on the runway 1.6 km from the SC laser. The SC beam quality is studied after atmospheric propagation through 1.6 km using a SWIR camera and is observed to be nearly diffraction limited with an M^2 value of <1.3. The SC laser is then used as the illumination source to perform diffuse spectral reflectance measurements of various

1559-128X/13/276813-11$15.00/0

samples kept 1.6 km from the laser. The SC reflectance measurements are compared with in-lab measurements performed using a quartz-halogen lamp and are seen to be in good agreement. Spectral stability measurements are performed at 1.6 km and show a relative variability of ~4%–8% depending on the atmospheric turbulence effects at the time of the measurements. Similar spectral stability measurements performed in-lab show a relative variability of <0.6%. The stability measurements indicate that atmospheric turbulence plays an important role and should be accounted for, when performing long distance measurements. The high average power, broad spectrum, and the convenience of an all-fiber integrated laser source with near diffraction limited beam quality makes the SC laser presented in this paper an attractive light source for active illumination in the SWIR wavelengths for long-distance remote sensing and hyperspectral imaging applications.

Light generation in the SWIR wavelengths (~1–2.5 μm) is beneficial for a number of applications in defense, healthcare, quality control, etc. [1–3]. The presence of atmospheric windows [4], where losses during propagation are minimal, coupled with the lower scattering compared to the visible wavelengths makes SWIR light sources particularly attractive for applications, such as remote sensing and light detection and ranging (LIDAR), which require long propagation distances through the atmosphere. In addition, at long ranges and under low visibility conditions, the signal-to-noise ratio (SNR) and image quality in the SWIR will be significantly better than in the near-IR and visible spectral bands [5]. A variety of detectors with high sensitivity are also available in this wavelength region [3]. High-power broadband sources are also attractive for airborne laser scanning measurements, a well-established technique for surface topography measurements as well as for 3D characterization of targets [6–9], and the addition of broadband spectral data to the intensity based scanning could potentially enable active imaging spectrometry in a single shot together with 3D topographic mapping capabilities [9].

Passive SWIR hyperspectral imagers have demonstrated the potential to detect targets of interest, but passive sources like solar illumination have several limitations, such as being confined to daytime operations, shadow regions, and being limited by weather conditions [10,11]. On the other hand, the spectra acquired with an active illumination source, such as SC lasers, are much less affected by illumination conditions or shadows and allow much more flexibility in measurement conditions [11]. In addition to the broad wavelength spectrum, the beam quality output stability and the average power of the illumination source are other important factors to consider for spectral measurements at long propagation distances. Infrared SC lasers have been studied in literature as potential sources for hyperspectral LIDAR [12–14], but most of these experiments were performed at distances of <100 m using low-power SC sources. Hyperspectral imaging devices generally require the illumination of large areas and, hence, high optical powers [15]. While steps can be taken to reduce the required power of illumination, this comes at the cost of lower operating SNR, reduced field of view of the sensor, and/or moving the sensor closer to the target [16]. With the recent development of mature gain fibers, high-power pump diodes, optical fibers of various materials, geometries, and dispersion profiles, it is now possible to construct a broadband high-power SC fiber laser platform for almost any wavelength region of interest [1] making SC laser sources attractive light sources for performing long-distance measurements. In addition, SC laser sources also have the advantages of conventional laser sources, can be focused or collimated easily, and are capable of producing near diffraction limited beams [17]. Thus, the combination of a broadband spectrum, high-average powers, and a near diffraction limited beam quality could potentially make SC lasers key enablers for a variety of practical long-distance spectral measurements, including airborne measurements.

In this article, we investigate the use of a high-power broadband SC laser as an active illumination source for remote sensing applications. Toward this goal, we study the beam quality, perform spectral reflectance, and spectral stability measurements using a packaged 5 W SWIR-SC laser prototype covering the wavelength region for ~1.55 to 2.35 μm. The laser is used as the active illumination source for field trials, where the SC laser placed on a 76 m tall tower at WPAFB is propagated through the atmosphere to a target on the runway 1.6 km away. The SC laser output leaving the tower is collimated using a parabolic mirror and is used to perform spectroscopy measurements of various targets kept 1.6 km away. The SC beam quality and output spectral stability are also studied after atmospheric propagation through 1.6 km. We demonstrate that SWIR-SC laser sources are capable of propagating long distances through the atmosphere with a nearly diffraction limited beam and good spectral stability. The results presented in this article suggest that SC lasers could potentially be used as active illumination sources for various long-distance remote sensing applications.

This article is organized as follows. In Section 2, we describe the setups used for the WPAFB field trials to characterize the SC laser and to perform spectral reflectance measurements. This is followed by a description of the 5 W SC laser prototype used in the 1.6 km field trials. The spectrum, power scaling and in-lab stability measurements are also presented in this section. Then, in Section 4, we present the results of the field trial starting with the SC beam quality. Next, the diffuse spectral reflectance measurements of various samples performed at 1.6 km using the SC laser as the illumination source are presented, followed by the SC output stability results after propagating 1.6 km through the atmosphere. Finally, in Section 5, we discuss the

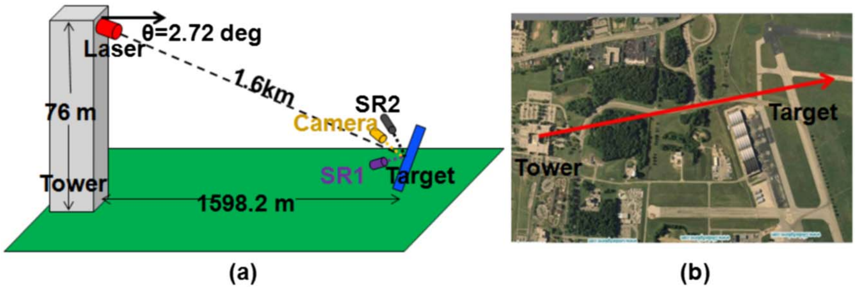

Fig. 1. (a) Diagram of tower-target test layout. (b) Map view of 1.6 km tower to ground path at WPAFB.

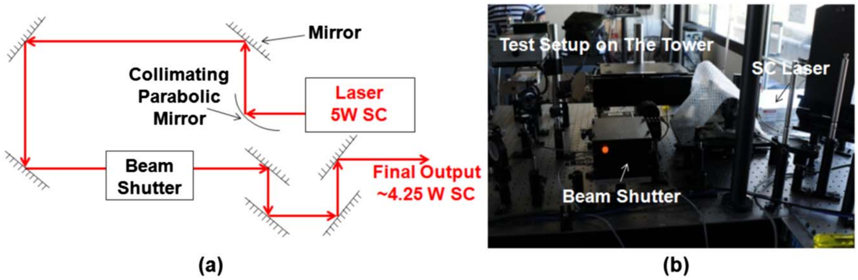

Fig. 2. (a) SC laser optical layout in the tower at the WPAFB. (b) SC laser in the tower at WPAFB.

experimental results, effects of atmospheric turbulence, and power scaling of the SC systems before ending with the summary.

2. Field Trial Setup

Field trials using the packaged SC prototype are conducted at the Air Force Research Labs (WPAFB) in Dayton, Ohio. The field trial layout is shown in Fig. 1. The SC laser is placed on a 76 m tall tower, and the collimated beam is propagated thorough the atmosphere to an 8 ft (2.44 m) × 8 ft (2.44 m) target panel kept 1.6 km away from the tower. The target panel consists of a plywood stand for placement of the materials of interest used in our measurement and is slightly tilted to create a normal surface with respect to the laser beam propagation angle of ~2.72°. The SWIR camera and the spectroradiometers (SR1 and SR2) for the various measurements are placed on the field close to the target. The tower-target beam alignment is verified by observing the reflected beam at the tower from a retro-reflecting mirror placed at the target site. All field measurements are performed after sunset to minimize the effects of solar illumination.

A. SC Laser Setup on Tower

A visible helium–neon laser beam is first used to verify the alignment between the tower and the target. The SC laser is then introduced into the beam path using a set of reflective mirrors. A beam shutter is used to block the beam, when required to make power measurements or background measurements at the target site. SC beam alignment is verified by observing the beam from a retroreflective mirror at the target site on an InGaAs camera on the tower. Figure 2 shows the laser layout on the tower. The final SC output power leaving the tower after the set of aligning mirrors is measured to be ~4.25 W. As shown in Fig. 1(a), the SC laser output is directed along a slant path to a target panel on the ground.

B. Beam Imaging Setup

The collimated SC beam image as projected on the target is measured using a SWIR camera (FLIR Systems SC6702, Massachusetts). The camera uses an indium antimonide detector array and covers the spectral range from ~1–5 μm. The detector resolution is specified as 640 × 512 with 15 μm pixels. The images are captured with a 4 ms integration time at 60 frames/s. Figure 3 shows the overhead layout of the camera used in the field trials. The camera is placed ~5.6 m from the target at ~10° from the target normal and measures the reflected laser light used to characterize the SC beam quality and the atmospheric turbulence effects.

C. Diffuse Spectral Reflectance Measurement Setup

Field spectroscopy measurements using the SC laser are performed using a grating based spectroradiometer SR1 (ASD Fieldspec 3, Colorado) with InGaAs

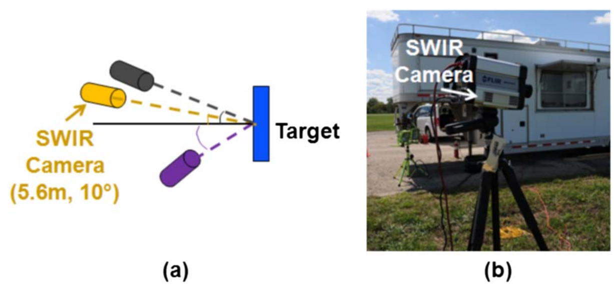

Fig. 3. (a) Overhead view of the beam quality measurement setup showing the position of the SWIR camera with respect to the target on the field. (b) Image of the SWIR camera.

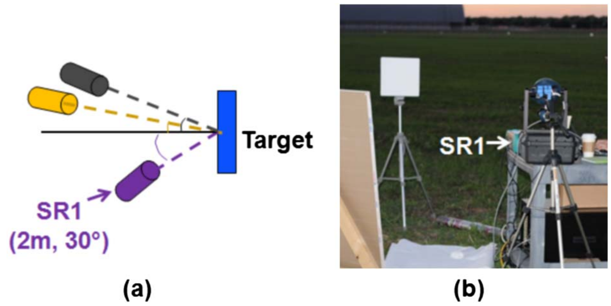

Fig. 4. (a) Overhead view of the field spectroscopy setup showing the position of the spectroradiometer SR1 with respect to the target on the field. (b) Image of SR1 used for the diffuse reflectance measurements.

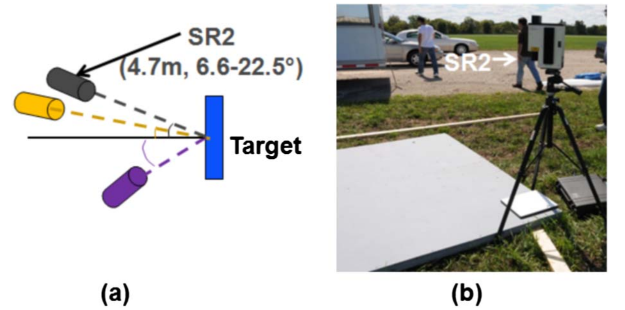

Fig. 5. (a) Overhead view of the spectral stability measurement setup showing the position of the spectroradiometer SR2 with respect to the target on the field. (b) Image of SR2 used for the spectral stability measurements.

detectors that cover the wavelengths from 1–2.5 μm. Figure 4 shows the overhead layout for SR1 used for the diffuse reflectance measurements in the field trials. The spectroradiometer is kept ~2 m from the target with the fiber optic receiver at an angle of ~30° with respect to the target normal. Materials with distinct reflectance spectra in the 1.5–2.5 μm are used for the spectral reflectance measurements and include Tyvek, a white cotton cloth, wallboard, plywood, blue tarp, and gray silt cloth.

To compare the reflectance data obtained using the SC laser, reference measurements are also performed in-lab for each of the samples using SR1 and a contact probe (ASD Hi-Brite contact probe, Colorado) with a built in illumination source (quartz-halogen based tungsten filament lamp) and a fiber-optic receiver attached to the probe that collects the reflected light. The illumination source in the contact probe provides relatively uniform illumination over the hemisphere, while the fiber optic measures the reflected illumination at a specific angle. The in-lab measurements using the contact probe provide an estimate of the material hemispherical directional reflectance (HDR).

D. Spectral Stability Measurements

The SC output stability at 1.6 km is measured using a spectroradiometer SR2 (SVC HR-1024, NY), with an InGaAs-array that covers the 1–1.89 μm region and an extended InGaAs array detector that covers the 1.89–2.5 μm spectral region. Figure 5 shows the overhead layout for SR2 used to measure the spectral output stability in the field trials. SR2 is kept ~4.7 m from the target at ~6.6–22.5° from the target normal. Using the spectroradiometer SR2, we measure the radiance spectra of the laser spot as projected on the target. The scan time for each measurement is 1 s. A measurement sequence with SR2 consists of 60 of these sample scans, each taken every 5 s (the timing is limited by the software). The relative variability is then calculated from the measurement sequences.

3. SWIR SC Laser

The optical layout of the all-fiber 5 W SWIR-SC laser used in the field trial is shown in Fig. 6(a) and consists of an amplified 1.54 μm laser source followed by a spectrum broadening fused silica fiber. The amplified 1.54 μm laser source consists of a 1542 nm seed laser diode that is driven by electronic circuits to provide a 0.5 ns pulse at variable repetition rates from ~20 MHz down to a few kilohertz. These pulses are amplified by two erbium ytterbium fiber amplifier (EYFA) stages designated as the preamplifier and the power-amplifier, respectively. The preamplifier consists of a ~2 m length of 12/130 μm (core/cladding diameter) EYFA pumped by a 940 nm diode laser, and the power amplifier consists of ~7 m length of 12/130 μm (core/cladding diameter) EYFA pumped by a ~25 W 940 nm diode. A 100 GHz bandpass filter is used after the preamplifier to filter out the amplified spontaneous emission. An in-line polarizer at the filter output ensures that the input to the power-amplifier is in the optimum polarization. The amplified 1.54 μm light is then spliced onto ~10 m length of 8/125 μm (core/cladding diameter), 0.125 NA, PM1550 fiber, where the interaction between the nonlinearity and the anomalous dispersion breaks up the quasi-CW input pulses into a train of solitons through modulation instability and significantly increases the peak power. These generated solitons will undergo further spectral broadening in the fiber due to a variety of nonlinear effects,

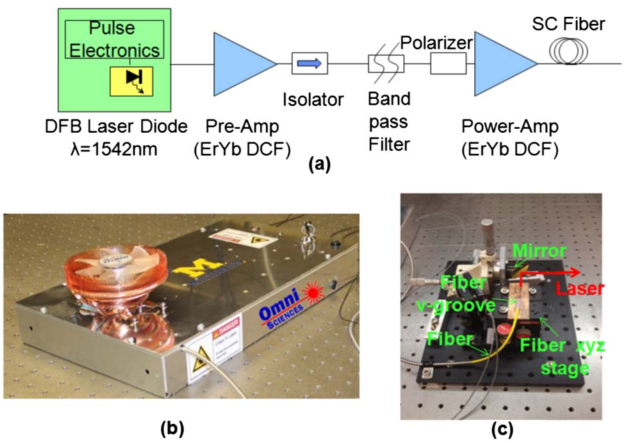

Fig. 6. (a) Optical layout of the all-fiber integrated 5 W SWIR SC laser. (b) Packaged 5 W SC laser prototype. (c) Collimation setup for the SC final output.

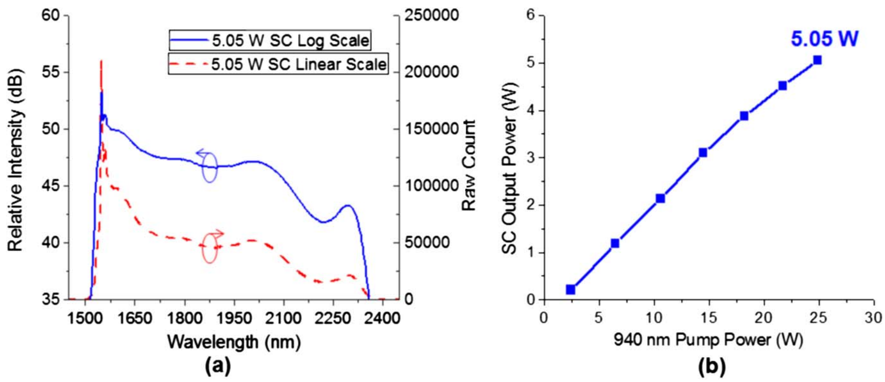

Fig. 7. (a) SC output spectrum spanning from ~1.55 to 2.35 μm with an average power of ~5 W across the continuum. The circles around each curve point to the corresponding Y axis. (b) SC output power scaling with 940 nm pump power in the power amplifier.

such as soliton self-frequency shift and Raman scattering, leading to the final SC output [1]. The in-line polarizer shown in Fig. 6 is a linear polarizer and the SC laser uses polarization maintaining fibers in the system. Therefore, the final SC output is also expected to be predominantly linearly polarized.

The SC laser is packaged in a box with dimensions of 10 in (0.25 m) × 17 in (0.43 m) × 2 in (0.05 m) and is shown in Fig. 6(b). The SC fiber output is also collimated and mounted on to a breadboard to allow for easy integration into the WPAFB setup for the field trials as shown in Fig. 6(c). The SC laser box and the collimation setup weigh ~7 lbs each. The SC collimation is achieved using a 90° off-axis parabolic gold coated mirror with a 25.4 mm focal length. The collimated beam diameter ($1/e^2$) at 1 m is measured to be ~6.5 mm.

Figure 7(a) shows the spectral output from the SC laser prototype corrected for the detector and grating response. The SC spectrum extends from ~1.55 to ~2.35 μm with a time averaged power of ~5.05 W in the entire continuum. The input comprises of 1.54 μm laser diode input pulses of ~0.5 ns duration at 8.3 MHz repetition rate. By pumping the power amplifier with ~25 W of 940 nm pump power in the counter propagation configuration, we are able to generate ~7 W of average power output around 1.54 μm. The pump (940 nm) to signal (1540 nm) efficiency at the output of the power-amplifier is observed to be ~28% and is typical of EYFA-based SC systems. The SC output power scaling with the power amplifier pump power is also shown in Fig. 7(b) and shows that ~25 W of 940 nm pump in the power-amplifier gives rise to the 5.05 W of final SC output in a ~10 m length of the PM1550 fiber.

Table 1. 5 W SWIR Amplitude Fluctuations at Different Wavelengths Measured In-Lab

Wavelength (nm)	% Fluctuation (Integration Time 100 ms)
1600	0.22
1800	0.23
2000	0.22
2200	0.57

The SC amplitude fluctuations are also measured in-lab at various wavelengths tuned using a spectrometer and lock-in amplifier. The SC relative variability is shown in Table 1. The measurements are performed at integration times of 100 ms (2 Hz sampling) using an InGaAs detector. The percent fluctuation at each wavelength is calculated as the ratio of the RMS sample to sample deviation and the mean of the measured amplitudes. The fluctuations are measured at 1.6, 1.8, 2, and 2.2 μm. The measured amplitude fluctuations show that the SC laser is stable with <0.6% fluctuation across the spectrum. The fluctuations measured in lab give an indication as to the stability of the SC laser in the absence of external factors like atmospheric turbulence.

The output power stability over long periods is another factor to consider in a practical light source for long-term measurements. We have performed power stability measurements for a continuous >43 h time period on the final system. The final power is measured at the fiber output without a collimating mirror. The results are shown in Fig. 8 and show an average power of ~5.09 W with a standard deviation of 0.012 W, corresponding to a fluctuation (standard deviation/average) of ~0.23%. The small variation is most likely due to the temperature fluctuations in the room temperature. Since our pump diodes are passively cooled, it is possible for the pump center wavelength to fluctuate with temperature, which could affect the final SC power level.

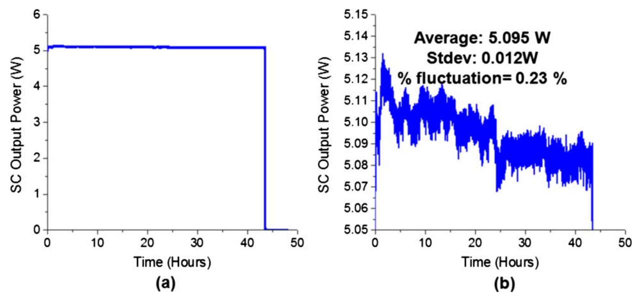

Fig. 8. (a) Long-term power stability measurements of the 5 W SC prototype before the collimating mirror. (b) Zoomed-in view of the stability measurements.

4. Field Trial Results

The results of the 1.6 km field trial are presented in this section beginning with the beam quality measurements, where the SC laser beam is seen to be nearly diffraction limited with an M^2 value of <1.3. Next we present the diffuse spectral reflectance measurements of various samples kept 1.6 km from the laser and illuminated using the developed SC laser prototype. The spectral features for the various samples from the spectroscopy measurements using the SC laser are also compared to in-lab measurements using a conventional quartz-halogen lamp and are seen to be in good agreement. Finally, the output spectral stability measurements after atmospheric propagation though 1.6 km are presented, where the relative variability is seen to be ~4%–8% depending on the atmospheric turbulence effects.

A. SC Beam Quality Measurements

Figure 9(a) shows a camera image of the collimated SC laser beam profile as projected on a target after 1.6 km of atmospheric propagation. Tyvek material is used as the target for these measurements since this material possesses high reflectance in this wavelength region. The profile shown is an average of 1000 frames measured using a 4 ms integration time. The beam diameter is measured as follows. First, the beam profile obtained using the camera is fit to a Gaussian profile. Then, the beam full width at half-maximum (FWHM) is measured from the Gaussian fit. Figure 9(a) shows a picture of the beam as projected on the target and Fig. 9(b) shows the beam profile through the beam cross section and the corresponding Gaussian fit.

At full power, the SC beam at 1.6 km is seen to be fairly Gaussian and symmetric (FWHM $x = 0.45$ m, FWHM $y = 0.47$ m), where the average FWHM is measured to be 0.46 m, corresponding to a $1/e^2$ diameter of ~0.78 m. From the measured beam diameter and the 1.6 km distance, the full angle beam divergence of the SC beam is then calculated to be $\theta_{\mathrm{SCBeam}} = 2 \times \tan^{-1}(0.39/1600) = 0.49$ mrad. For an ideal Gaussian beam at the SC average wavelength of ~2 μm and a similar collimated beam waist diameter of ~6.5 mm as the SC beam, the full-angle beam divergence can be calculated as $\theta_{\mathrm{Ideal}} = 2 \times \lambda/(\pi \times w_0) = 2 \times 2 \times 10^{-6}/(\pi \times 3.25 \times 10^{-3}) = 0.39$ mrad.

The M^2 factor is a common measure of the laser beam quality and is used to quantify the ratio of divergence of the actual laser beam to an ideal Gaussian beam. An ideal Gaussian beam has an M^2 value of 1. Thus, the M^2 value indicates how close in divergence, and hence, diffraction limited the laser beam is, compared to an ideal Gaussian beam. The SC M^2 value is calculated as the ratio of the SC beam divergence and the ideal Gaussian beam divergence, and is seen to be $\theta_{\mathrm{SCBeam}}/\theta_{\mathrm{Ideal}} = \sim 0.49/0.39 = \sim 1.26$. Thus, the calculated SC M^2 value of ~1.26 from the measurements at 1.6 km indicates that the SC beam is nearly diffraction limited. Additional M^2 measurements performed at ~17.5 m using an aperture and a power meter also show M^2 values of <1.3 as well.

The laser beam shape/profile at 1.6 km has also been compared with the theoretical distribution assuming a Gaussian beam propagation. The measured and the corresponding fit of the beam are compared with the theoretical profile for the average operating wavelength of 2 μm and a full angle laser divergence of 0.5 mrad. The estimated $1/e^2$ spot radius for the horizontal and vertical beam profile at 1.6 km are 0.38 and 0.40 m, respectively, both of which are seen to agree well with the theoretical spot radius of 0.40 m [18].

B. SC Spectral Reflectance Measurements at 1.6 km

After verifying the SC beam propagation through 1.6 km, the tower based SC laser is used as an illumination source to perform spectral reflectance measurements of various materials, to determine if the laser provides enough signals at ~1.6 km to retrieve spectral information from the targets. The spectral reflectance measurements are also compared to in-lab measurements performed using a contact probe with a built in illumination source and a fiber-optic receiver described in Section 2.C. The spectroradiometer SR1 is used for both the field and in-lab spectral reflectance measurements. To perform reflectance retrieval measurements using the spectroradiometer SR1, a spectrally flat "white" reference material is required. In our experiments,

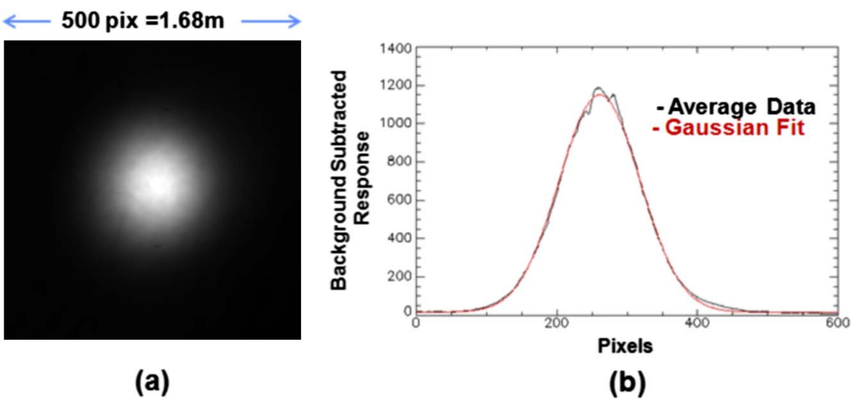

Fig. 9. SC laser (EYFA system) beam profile measurements at ~1.6 km, 1000 frame average. (a) Camera image of the beam and (b) Gaussian fit and beam width measurement.

a 2 ft (0.61 m) × 2 ft (0.61 m) spectralon (Labsphere SRT-99-240 Reflectance Target, New Hampshire), calibrated over the wavelength range from 250 to 2500 nm (reported at 50 nm intervals) is held at the same illumination/viewing angle as the various targets and is used as the white reference.

Figure 10 shows the retrieved spectral reflectance for the various samples measured using the SC laser averaged over at least 30 measurements for each sample, and the corresponding in-lab reflectance measurements. The in-lab measurements are collected in a more controlled setting using a quartz-halogen filament lamp as the light source and a fiber-optic contact probe. The SC data in the wavelengths from ~1.8–1.95 μm are absorbed by the water in the atmosphere and have been removed from the figure.

As seen in Fig. 10, the spectral reflectance curves for the various samples agree closely with the lab measurements, especially with respect to the spectral shape of the curves. For many of the materials in Fig. 10, a reflectance offset exists between the lab measurements and the SC laser measurements. The field reflectance measurements are performed with the SR1 fiber optic receiver positioned at approximately the same angle (with respect to the target normal) as the in-lab measurements. Since the SC laser is much more directional than the illumination conditions used for the in-lab measurements, the estimated reflectance is not quite HDR. The reflectance offset between the in-lab and the SC laser measurements is likely the result of bidirectional reflectance distribution function of non-Lambertian target surfaces and possible differences that exist between the illumination/viewing geometry [19] for the lab and field measurements.

The nature of the spectral offset between the SC measurements and the reference measurements in Fig. 10 is further explored for three samples: blue tarp, plywood, and gray silt cloth. The spectroradiometer SR1 used for the spectral reflectance measurements uses a grating with a linear 512 element detector for the visible-near IR (0.3–1 μm), an oscillating grating and a detector for SWIR band1 (1–1.83 μm) and another grating/detector pair for the SWIR band 2 (1.8.–2.5 μm). Since our experiments with the SC laser cover the ~1.5 μm × 2.3 μm, we use two of the three spectral regions covered by SR1. The spectral offset for the samples measured in Fig. 10 using the SC appear to be a fairly constant offset compared to the reference spectrum, which suggests that the offset is likely independent of the wavelength. For example, Fig. 11 shows the spectral measurements for three samples, blue tarp, plywood, and gray silt cloth that have been corrected using constant factors in each wavelength band to match the corresponding reference spectrum in that band. As we can see in Fig. 11, the majority of the spectral offset between the SC and the reference spectra is accounted for with a constant correction factor. Other possible reasons for the additional offset could be wavelength dependent, such as scattering arising from the sample surface features (roughness, surface profile, etc.), changes in the

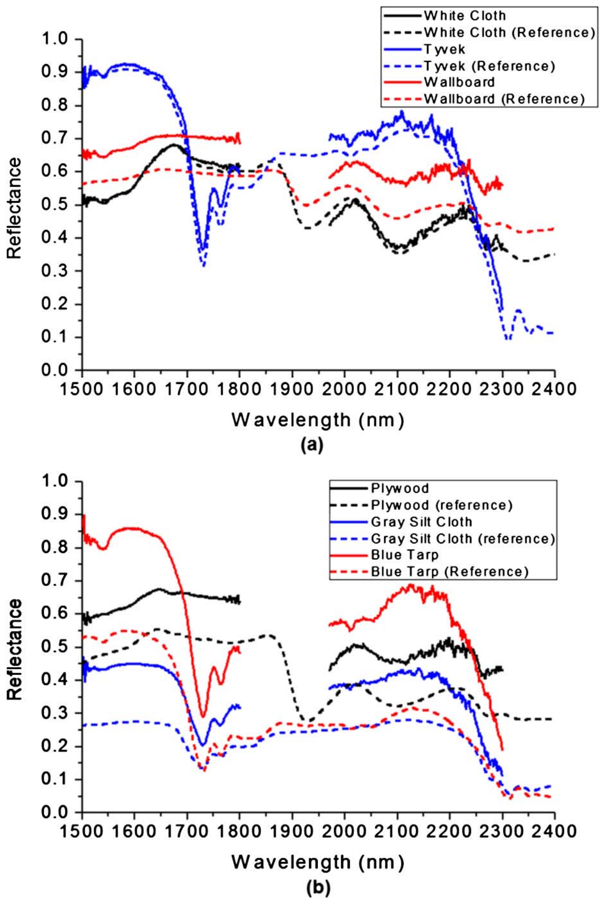

Fig. 10. Spectral reflectance measurements at ~1.6 km using the SC laser (solid lines) and their comparison to in-lab measurements performed using a quartz-halogen lamp (dashed lines). (a) Retrieved reflectance of white cloth, Tyvek, and wallboard. (b) Retrieved reflectance of plywood, gray silt cloth, and blue tarp.

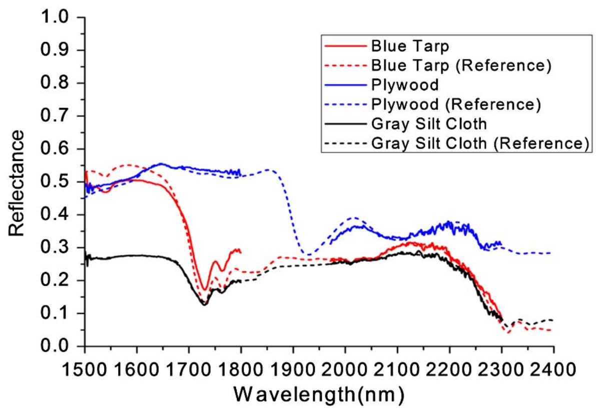

Fig. 11. Reflectance spectra for blue tarp, plywood, and gray silt cloth corrected with constant offset factors in each of the SWIR wavelength bands. The SC measurements overlap fairly well with the reference measurements after the applications of constant offset factors in each on the SWIR wavelength bands.

incident/reflection angle of the illumination, atmospheric effects, etc. However, these factors appear to play a minor role in our current measurement configuration, since most of the SC spectral features overlap fairly well with the reference spectra after the application of just a constant offset factor.

C. SC Output Stability Measurements

For the SC source to be useful as a broadband illuminator for various applications, it should provide stable irradiance. Using spectroradiometer SR2, we measure the radiance spectra of the laser spot as projected on the target at 5 s intervals (the timing is limited by the spectroradiometer software). The scan time for each measurement was 1 s, during which the spectroradiometer continuously collected and averaged data. Figure 12(a) shows a sample measurement sequence of 60 such scans acquired using SR2. To quantify the variability, we calculate the RMS sample-to-sample difference in radiance at each wavelength band and divide by the mean radiance spectrum. Figure 12(b) shows the variability profiles for seven measurement sequences over two days. Radiometric variations in the field experiment include atmospheric effects that are not present at significant levels in the lab. The radiometric variability at 1.6 km is observed to be between ~4% and 8%, depending upon the turbulence conditions.

The refractive index structure parameter (Cn^2) value is often used as a measure of atmospheric turbulence and is a function of the local differences in temperature, moisture, and wind velocity. The Cn^2 values observed in the atmospheric surface layer generally range from 10^{-12} to 10^{-16} $m^{-2/3}$, where higher values indicate a higher atmospheric turbulence [20]. The time stamps on the SC measurements are correlated to the scintillometer data collected by Air Force Research Lab to extract the (Cn^2) value corresponding to each SC measurement sequence. Although the Cn^2 values are measured at 880 nm, which is outside of the SC range, there is a general correlation between the Cn^2 and the relative signal variability. As seen in Fig. 12(b), the SC relative variability seems to follow this trend as well, where higher variability is associated with higher Cn^2 value. Thus, atmospheric turbulence is an important factor to consider in measurements involving propagation through long distances in the atmosphere.

Compared to the in-lab fluctuations of <0.6%, the fluctuations at 1.6 km range from ~4% to 8% depending on the turbulence conditions. The atmospheric turbulence affects SC output stability and adds an additional noise term that must be accounted for when trying to predict the operational performance of light sources [18]. Figure 13(a) shows a single frame camera image of the 5 W SWIR beam at ~1.6 km, where the effects of atmospheric turbulence on the beam are evident. Some of the possible ways to mitigate the turbulence effects on beam quality are averaging of multiple camera frames and performing background subtraction. As an example, Fig. 13(b) shows a 1000 frame average of the same laser beam after background subtraction, where the beam is seen to be much more stable. Thus, the effects of atmospheric turbulence must be considered in the laser system designs [21] used for long distance remote sensing applications. A variety of techniques, such as using adaptive optics, deformable mirrors, beam dithering etc., have also been investigated in literature to mitigate the effects of atmospheric turbulence in laser beam propagation [22–24].

5. Discussion

SC laser sources cover a broad wavelength region, can be easily collimated, provide near diffraction limited beams, and are capable of producing high-average power outputs. Therefore, SC lasers are an attractive candidate for active illumination for hyperspectral imaging and other remote sensing applications. The beam quality measurements in Section 4.A show that the developed SC laser is capable of producing a nearly diffraction limited beam with an M^2 value <1.3. The spectral reflectance measurements at 1.6 km, shown in Section 4.B, indicate that the SC laser can be reliably used for spectroscopy measurements over long distances. The SC spectral stability at 1.6 km is seen to vary between 4% and 8% depending on the atmospheric

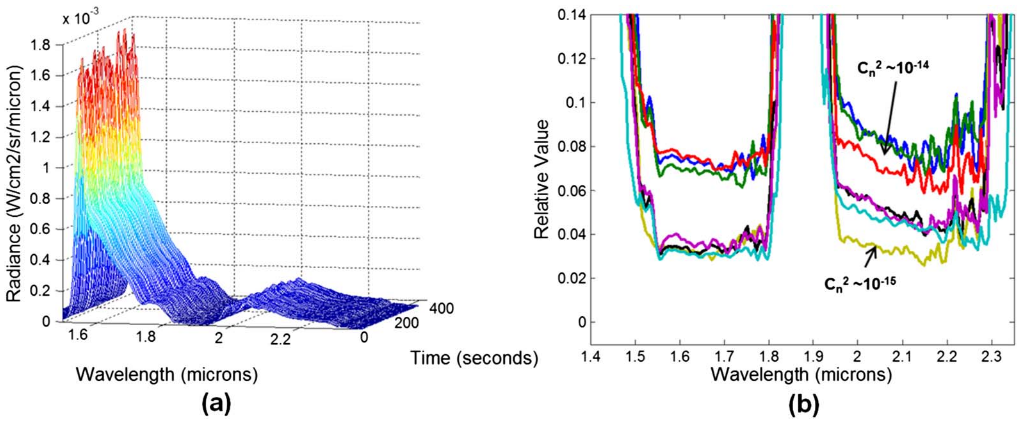

Fig. 12. (a) Sample measurement sequence of radiance spectra at 1.6 km range. (b) Relative scan-to-scan variability for seven field measurements.

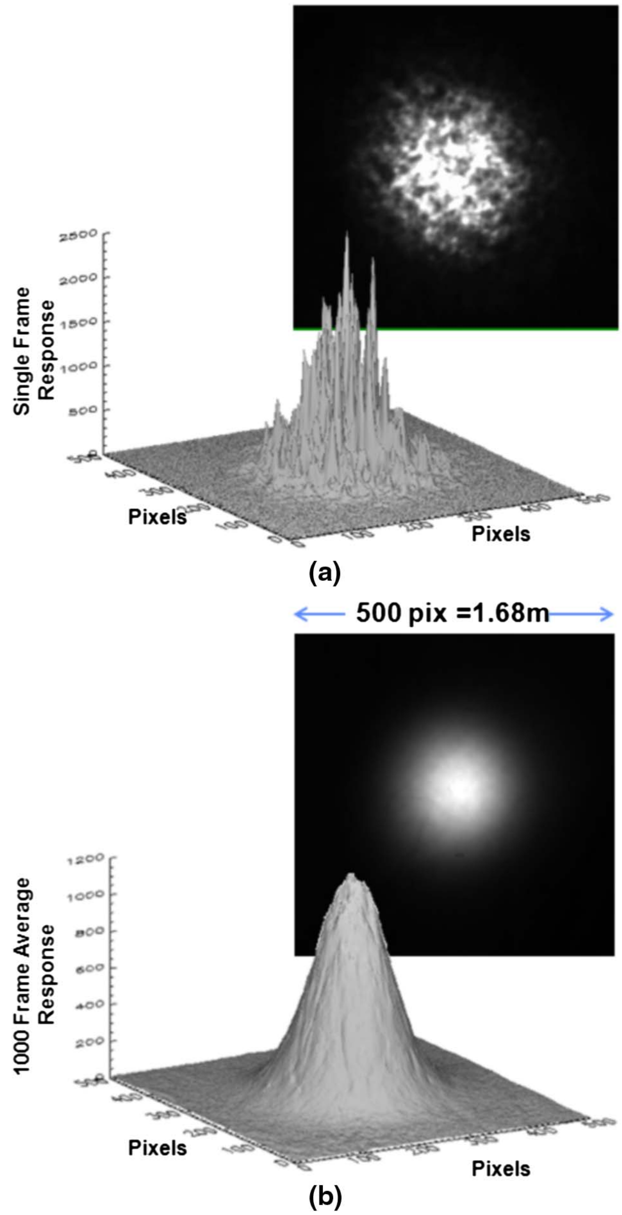

Fig. 13. (a) Single frame image of the SC laser beam at ~1.6 km showing effects of atmospheric turbulence. (b) 1000 frame average of the same beam with background subtraction showing a much smoother beam profile.

turbulence effects, while in-lab measurements show a relative variability of <0.6% and suggests that the turbulence plays an important role in the stability of the SC laser after propagation through the atmosphere and is the likely contributor to the higher SC fluctuations measured at 1.6 km.

The measured beam diameters and the M^2 values at 1.6 km shown in Section 4.A depend strongly on the collimating optics used, and how well collimated the beam is. In our case, we use a gold coated parabolic mirror to collimate the SC beam and to avoid any effects of chromatic aberration, but it was not possible for us to easily optimize the collimation during the field trial due to time limitations and lack of a real-time feedback process. The SC laser presented in this article uses single mode fibers for the SC generation process. As such, the beam quality is expected to be good with an M^2 value close to the ideal value of 1. High-power single mode fiber lasers have been reported with M^2 values <1.1 [25]. High power broadband SC lasers have also been reported in literature with M^2 values ranging from 1.06 to 1.08 [26].

The spectral reflectance measurements in Section 4.B are performed with the target kept ~1.6 km from the SC laser, but the spectrometers and detectors are kept at small distances (<5 m) from the target to receive sufficient signal levels. While this is a great preliminary proof of concept, in an actual remote sensing scenario, the detector will also be kept at long distances from the target. Thus, a higher-power SC laser will have to be used to ensure that a sufficient signal is received at the detector. Ultimately, the goal is to perform long-distance measurements on the ground, tower, or even airborne measurements using the SC lasers as the active illumination source. Since, solar illumination is a commonly used source for passive measurements, we can estimate the approximate SC power levels required to match the solar irradiance on the ground surface. Solar radiation reaching the earth's surface depends on a variety of factors, such as the location, atmospheric conditions, cloud cover, aerosol content, ozone layer conditions, time of day, Earth/Sun distance, solar radiation and activity. The total terrestrial solar irradiance in the ~1.5–1.8 μm and the 2–2.5 μm wavelength regions are ~75 and ~25 W/m^2, respectively [27]. Using the full angle divergence for the SC laser at 1.6 km to be ~0.49 mrad, as measured in Section 4.A, we estimate the corresponding beam diameters at 1.6 and 3.05 km (10,000 ft) to be ~0.78 and ~1.49 m, respectively. We can then calculate the approximate SC power required to mimic the solar irradiation at 1.6 and 3.05 km (10,000 ft), assuming negligible attenuation during propagation. The calculated SC power levels are shown in Table 2. The estimations in Table 2 show that to match the 75 W/cm^2 at 1.6 and 3.05 km, we would need SC powers of ~36 and ~131 W, respectively, in the 1.5–1.8 μm wavelength region. Similarly, the required power levels in the 2–2.5 μm wavelength region at 1.6 and 3.05 km are estimated to be ~12 and ~44 W, respectively.

For the field trial presented in this article, the SC beam travels through a significant length of the atmosphere, which increases the effects of turbulence. In an airborne measurement, the beam will most likely be normal to the surface and propagate

Table 2. Approximate Values for the SC Power Required to Match the Solar Irradiance at ~1.6 and ~3.05 Km

Wavelength (μm)	Solar Irradiance (W/m^2)	SC Power Required at ~1.6 km	SC Power Required at ~3.05 km
1.5–1.8	75	36 W	131 W
2–2.5	25	12 W	44 W

through a thinner atmospheric section, which would reduce the turbulence effects. To understand the potential improvement in turbulence, we estimate the ratio of turbulence strength (as a function Cn^2) at 3.05 km (10,000 ft) collected at an elevation of 90° (nadir) to that in our current measurements at 1.6 km collected at an elevation of 2.72° using the Tatarski approximation equation [28] $C_n^2 \approx C_{n0}^2 h^{-4/3}$, where h is the height through the turbulent medium and C_{n0} is the refractive index structure coefficient at the surface. Substituting $h = r\,\sin(\theta)$, where r is the line of sight propagation distance and θ is the elevation angle in radians, we can then estimate C_n^2 as

$$C_n^2(R,\theta) = C_{n0}^2 \int_{r0}^{r1} (r\,\sin(\theta))^{-4/3}\mathrm{d}r$$

$$r_0 = \frac{h_0}{\sin(\theta)}, \qquad r1 = \frac{h_0}{\sin(\theta)} + R,$$

h_0 is the height of the target assumed to be ~1 m

$$C_n^2(R,\theta) = 3C_{n0}^2(\sin(\theta))^{-4/3}\left[\left(\frac{h_0}{\sin(\theta)}\right)^{-1/3} - \left(\frac{h_0}{\sin(\theta)} + R\right)^{-1/3}\right] \times \frac{C_n^2(3.05\ \mathrm{km}, 90°)}{C_n^2(1.6\ \mathrm{km}, 2.72°)} \approx 0.06. \tag{1}$$

Thus, the ratio of the turbulence strength at 10,000 ft (3.05 km) at an elevation of 90° to our measurements at 1.6 km at an elevation of $2.72°[Cn^2(3.05\ \mathrm{km}, 90°)/Cn^2(1.06\ \mathrm{km}, 2.72°)]$ is calculated using Eq. (1) to be ~6%. Therefore, in an airborne measurement setup with the beam normal to the surface of interest, the effect of turbulence is estimated to be ~6% of our measured results. Given our measured relative SC variability of 4%–8% at 1.6 km, the equivalent variability for the nadir at 3.05 km is then estimated to be ~0.2%–0.5%.

While the SC laser presented in this article covers the ~1.55–2.35 μm region of the SWIR band, the SC generation architecture presented in this paper allows for the customization of the various components to potentially generate an SC across the entire SWIR band (~1–2.5 μm), by choosing the appropriate gain and SC generation fibers [1]. The SWIR wavelength band is especially attractive for SC lasers, since this wavelength region allows the use of standard fused silica fibers for SC generation, which are generally much easier to handle and have a higher-power damage threshold compared to other fibers, such as fluoride fibers used for the mid-IR regimes [17]. As shown in Section 3, we have developed an all fiber 5 W SC laser covering the SWIR bands from ~1.55 to 2.35 μm, after which the long wavelength edge of the fused silica fiber based SC laser is limited by the soaring absorption of silica glass [29].

High average-power SC lasers are potential key enablers for practical long distance/airborne hyperspectral imaging and other remote sensing applications, where speed and signal quality play an important role. For the SC laser presented here, the power scaling is limited by the available 940 nm pump power. The maximum average power handling capability of the fiber may be limited also when the temperature of the fiber core rises close to its melting point. By increasing the pump powers, and with better thermal management and heat dissipation techniques, it should be possible to further scale up the average power output of these all-fiber SWIR SC lasers. For example, Xia *et al.*, estimate the damage threshold in a standard fused silica single-mode fiber based SC system, where the fiber dimensions are comparable to our current system, to be >60 W [17]. An advantage of SC laser architecture presented here is the ability to scale up the average output power, while maintaining the same spectral extent, by increasing the repetition rate and the corresponding pump powers. For example, we recently reported an SC laser using similar architecture, where the average SC output power is scaled up from 5 to 25.7 W in a spectrum covering the SWIR band from ~2 to 2.5 μm, by increasing the repetition rate from ~0.2 to ~1.1 MHz and using a power amplifier pumped with ~112 W of pump power [30]. We also show that this SC laser platform is truly power scalable in that the SC maintains a near constant spectrum, good beam quality, and low-output variability as the average output power is scaled up, making the SC lasers potentially ideal illumination sources for long-distance remote sensing and hyperspectral imaging applications.

The results presented in this manuscript suggest that the spectral stability is sufficient for down-looking spectral remote sensing. The transmitter variability is sufficiently low that the primary noise sources are expected to be the turbulence-induced variability and the receiver noise. As we show in our calculations using Eq. (1), the turbulence effects are expected to be much less when transmitting from directly above (such as airborne measurements), on the order of the lab-measured transmitter variability. The more significant limiting factor for a round-trip measurement is the output power. At 5 W the area coverage of a remote sensing system is limited because the beam will need to be concentrated on a small area long enough for the receiver to collect an adequate signal. In the future, we plan on increasing the output power and performing remote sensing measurements with the laser and detector collocated at long distances.

6. Summary

We present the results of a field trial performed using a developed SWIR-SC laser source for active remote sensing. An all-fiber 5 W SWIR SC laser covering the ~1.55–2.35 μm wavelength band is developed and placed on a 76 m tall tower at WPAFB and propagated through the atmosphere to a target on the runway 1.6 km away. Field trials are performed to

characterize the SC beam quality and output stability after 1.6 km of atmospheric propagation. The developed SC laser has a near diffraction limited beam with an M^2 value of <1.3, when measured using a SWIR camera. The SC laser is also used as an active illumination source to perform spectral reflectance measurements of various samples at 1.6 km, and the SC measurements are seen to be in good agreement with in-lab measurements performed using a conventional quartz-halogen lamp. The SC output variability at 1.6 km is measured to be 4%–8% and is seen to depend on the atmospheric turbulence effects. In the absence of turbulence, the SC stability measurements in-lab show a relative variability of $<6\%$. We discuss some of the possible techniques to improve the beam quality and mitigate the turbulence effects, as well as provide a preliminary estimation of the SC power levels applicable for long-distance remote sensing applications. The high-average power, broad spectrum and the convenience of an all-fiber integrated laser source with near diffraction limited beam quality makes the SC lasers presented here an attractive light source for active illumination in the SWIR wavelengths for long distance hyperspectral imaging and remote sensing applications.

This project was funded by NGA and AFRL. The authors would like to thank David Carter, Jim Tice, and Michael Folts at the Physics Instrument Shop for their help in machining parts of the laser prototype. We also thank Michael Wager, Tyler Masterson, and Bruce Smotherman for their help with the field-trial setups at WPAFB. Dr. Mohammed N. Islam is a professor in the Electrical and Computer Engineering Department and the Department of Internal Medicine at the University of Michigan and is also the Founder, Chief Technology Officer, and consultant to Omni Sciences Inc.

References

1. V. V. Alexander, O. P. Kulkarni, M. Kumar, C. Xia, M. N. Islam, F. L. Terry, Jr., M. J. Welsh, K. Ke, M. J. Freeman, M. Neelakandan, and A. Chan, "Modulation instability initiated high power all-fiber supercontinuum lasers and their applications," Opt. Fiber Technol. **18**, 349–374 (2012).
2. S. D. Jackson, "High-power fiber lasers for the shortwave infrared," Proc. SPIE **7686**, 768608 (2010).
3. M. P. Hansen and D. S. Malchow, "Overview of SWIR detectors, cameras, and applications," Proc. SPIE **6939**, 69390I (2008).
4. J. H. Taylor and H. W. Yates, "Atmospheric transmission in the infrared," J. Opt. Soc. Am. **47**, 223–225 (1957).
5. R. N. Lane, "The SWIR advantage," Proc. SPIE, **2555**, 246–254 (1995).
6. K. Kraus and N. Pfeifer, "Determination of terrain models in wooded areas with airborne laser scanner data," ISPRS J. Photogramm. Remote Sens. **53**, 193–203 (1998).
7. J. Hyyppä, O. Kelle, M. Lehikoinen, and M. Inkinen, "A segmentation based method to retrieve stem volume estimates from 3-D tree height models produced by laser scanners," IEEE Trans. Geosci. Remote Sens. **39**, 969–975 (2001).
8. N. Haala and C. Brenner, "Extraction of buildings and trees in urban environments," ISPRS J. Photogramm. Remote Sens. **54**, 130–137 (1999).
9. S. Kaasalainen, T. Lindroos, and J. Hyyppä, "Toward hyperspectral LIDAR: measurement of spectral backscatter intensity with a supercontinuum laser source," IEEE Geosci. Remote Sens. Lett. **S4**, 211–215 (2007).
10. G. Bishop, I. V. Veiga, M. Watson, and L. Farr, "Active spectral imaging for target detection," in proceedings of the *4th EMRS DTC Technical Conference*, Edinburgh (2007).
11. M. L. Nischan, R. M. Joseph, J. C. Libby, and J. P. Kerekes, "Active spectral imaging," Lincoln Lab. J. **14**, 131–144 (2003).
12. T. Hakala, J. Suomalainen, S. Kaasalainen, and Y. Chen, "Full waveform hyperspectral lidar for terrestrial laser scanning," Opt. Express **20**, 7119–7127 (2012).
13. Y. Chen, E. Räikkönen, S. Kaasalainen, J. Suomalainen, T. Hakala, J. Hyyppä, and R. Chen, "Two-channel hyperspectral LIDAR with a supercontinuum laser source," Sensors **10**, 7057–7066 (2010).
14. R. Ceolato, N. Riviere, and L. Hespel, "Reflectances from a supercontinuum laser-based instrument: hyperspectral, polarimetric, and angular measurements," Opt. Express **20**, 29413–29425 (2012).
15. C. R. Howle, D. J. M. Stothard, C. F. Rae, M. Ross, B. S. Truscott, C. D. Dyer, and M. H. Dunn, "Active hyperspectral imaging system for the detection of liquids," in Proc. SPIE **6954**, 69540l (2008).
16. G. A. Shaw and H.-H. K. Burke, "Spectral imaging for remote sensing," Lincoln Lab. J. **14**, 3–28 (2003).
17. C. Xia, Z. Xu, M. N. Islam, J. Fred, L. Terry, M. J. Freeman, A. Zakel, and J. Mauricio, "10.5 w time-averaged power mid-IR supercontinuum generation extending beyond 4 μm with direct pulse pattern modulation," IEEE J. Sel. Top. Quantum Electron. **15**, 422–434 (2009).
18. J. Meola, A. Absi, J. D. Leonard, A. I. Ifarraguerri, M. N. Islam, V. V. Alexander, and J. A. Zadnik, "Modeling, development, and testing of a shortwave infrared supercontinuum laser source for use in active hyperspectral imaging," Proc. SPIE **8743**, 87431D (2013).
19. M. Kumar, M. N. Islam, F. L. Terry, Jr., M. J. Freeman, A. Chan, M. Neelakandan, and T. Manzur, "Stand-off detection of solid targets with diffuse reflection spectroscopy using a high-power mid-infrared supercontinuum source," Appl. Opt. **51**, 2794–2807 (2012).
20. A. Tunick, N. Tikhonov, M. Vorontsov, and G. Carhart, "Characterization of optical turbulence (cn2) data measured at the ARL A_LOT facility," ARL-MR-625 (2005).
21. J. Davis, "Consideration of atmospheric turbulence in laser systems design," Appl. Opt. **5**, 139–148 (1966).
22. M. C. Roggemann and D. J. Lee, "Two-deformable-mirror concept for correcting scintillation effects in laser beam projection through the turbulent atmosphere," Appl. Opt. **37**, 4577–4585 (1998).
23. X.-C. Tan, Z.-C. Wu, and Z. Liang, "Effect of adaptive optical system on the capability of LIDAR detection in atmosphere," Proc. SPIE **7284**, 72840G (2009).
24. D. N. Loizos, L. Liu, P. P. Sotiriadis, G. Cauwenberghs, and M. A. Vorontsov, "Integrated multi-dithering controller for adaptive optics," Proc. SPIE **6708**, 67080B (2007).
25. B. Shiner, retrieved http://www.photonics.com/Article.aspx?AID=25158.
26. X. Hu, W. Zhang, Z. Yang, Y. Wang, W. Zhao, X. Li, H. Wang, C. Li, and D. Shen, "High average power, strictly all-fiber supercontinuum source with good beam quality," Opt. Lett **36**, 2659–2662 (2011).
27. "Introduction to solar radiation," retrieved http://www.newport.com/Introduction-to-Solar-Radiation/411919/1033/content.aspx.
28. N. S. Kopeika, *A System Engineering Approach to Imaging, Technology & Engineering* (SPIE, 1998).
29. T. Izawa, N. Shibata, and A. Takeda, "Optical attenuation in pure and doped fused silica in their wavelength region," Appl. Phys. Lett. **31**, 33–35 (1977).
30. V. V. Alexander, Z. Shi, M. N. Islam, K. Ke, M. J. Freeman, A. Ifarraguerri, J. Meola, A. Absi, J. Leonard, J. Zadnik, A. S. Szalkowski, and G. J. Boer, "Power scalable >25 W supercontinuum laser from 2–2.5 micron with near diffraction limited beam and low output variability," Opt. Lett. **38**, 2292–2294 (2013).